2013 IEEE/RSJ International Conference on
Intelligent Robots and Systems (IROS)
November 3-7, 2013. Tokyo, Japan

Series-Parallel Elastic Actuation (SPEA) with intermittent mechanism for reduced motor torque and increased efficiency

Glenn Mathijssen[1], Branko Brackx, Michael Van Damme, Dirk Lefeber, and Bram Vanderborght

Abstract— **Future robots will need to perform complex and versatile tasks comparable to those of humans. Due to the unavailability of suitable actuators, however, novel intelligent and agile robots are often restricted in their performances and development. The limited output torque range and low energy efficiency of current robotic actuators are the main bottlenecks. We have developed a SPEA with intermittent mechanism that addresses these problems. The SPEA is a novel compliant actuator concept that enables variable recruitment of parallel elastic elements and adaptive load cancellation. This paper describes how a SPEA lowers the motor torque and increases the energy efficiency. Experiments on the first proof of concept set-up endorse the practicability of the SPEA concept and the modeled trend of a lowered motor torque and increased energy efficiency. We expect that features of the biologically inspired SPEA with intermittent mechanism will prove exceedingly useful for robotics applications in the future.**

I. Introduction

The term 'soft robotics' has been introduced for all the novel requirements of safety and energy-efficiency of robots where a strong collaboration between robots and humans is targeted [1]. This trend started with the publications by Hogan on impedance control [2] that introduced compliant behavior of motors by software control, and the introduction of compliant elements in the hardware of the Series Elastic Actuator (SEA) of Pratt [3]. The introduction of spring elements in the actuation of robots was inspired by biology, for example the work of Alexander [4] explains the important role of biological springs in animals and humans. The next important step was to make the stiffness (and damping) of the compliant element adjustable in so called Variable Impedance Actuators (VIA) [5] like AWAS II [6], vsaUT-II [7], etc. Despite of the advances in both stiff and bio-inspired compliant actuation schemes, the current actuation technology is often still inadequate for (mostly novel) applications with versatile output requirements and required autonomy (e.g. exoskeletons, humanoids, prostheses, manipulators, etc.). The main problem is that actuators (servomotor, gearbox and possibly springs) with a wide output profile (torque, velocity and power) are generally bulky, heavy and energy inefficient [8] [9].

All authors are with the Robotics & Multibody Mechanics Research Group, Faculty of Mechanical Engineering, Vrije Universiteit Brussel, 1050 Elsene, Belgium. http://mech.vub.ac.be/robotics
[1] Corresponding author: Glenn.Mathijssen@vub.ac.be

This paper is organized as follows: after the problem analysis of DC motors in robotics in section II, the SPEA with intermittent mechanism concept is introduced in section III. The Proof of Concept (PoC) set-up and its theoretical model are introduced in section IV, followed by the experimental results on this PoC in section V.

II. DC Motors in robotics

Traditional DC motors are widely used in robotics. The technology of DC motors and their control advanced over 2 centuries so that their development is assumed to be mature. In robotics, DC motors are favored for their high maximum efficiency, high power-to-weight ratio and the convenience of electricity as a power source. Furthermore, the extra payload is small and they are inexpensive. The most basic model of a DC motor is describing the equilibrium state (i.e. constant voltage V, motor torque T_m and motor speed ω_m) and given by (1):

$$V = RI + k_b\omega_m \quad and \quad T_m = k_t I - \nu\omega_m \tag{1}$$

Although the maximum efficiency of a DC motor is generally high (>95%), the region in which this high efficiency occurs is limited. Especially at low speed and high torque the efficiency drops drastically. This is clarified by (2), i.e. the efficiency as a function of speed and torque, and the mesh plotted in Fig. 1:

$$\eta(\omega_m, T_m) = \frac{T_m\omega_m}{\left(R\frac{T_m+\nu\omega_m}{k_t} + k_b\omega_m\right)\frac{T_m+\nu\omega_m}{k_t}} \tag{2}$$

The required motor parameters of the HITEC HS-5955TG servomotor, used in the experiments in section V of this paper, are as follows: nominal voltage V_{nom}=6 V, gear ratio r=347:1, terminal resistance R=1.4 Ω, stall current I_{stall}=4.2 A, stall torque T_{stall}=2.35 Nm, no load speed $\omega_{no\ load}$=2422 $\frac{rad}{s}$, no load current $I_{no\ load}$=0.3 A and estimated gearbox efficiency of 55%. These parameters allow to calculate the viscous damping ν, and the motor constants k_t and k_b. As can be seen in Fig. 1, the region with acceptable efficiency is in the low torque region at about $\frac{1}{8}$ of the stall torque. As a result, DC motors should be designed according to their application so that the motor torque is in the high efficiency region. Traditionally this is done by high reduction gearboxes, with the downside of limiting the speed, increasing the mass and increasing the losses. A second solution is to select a heavier motor, since [10] showed that the mass

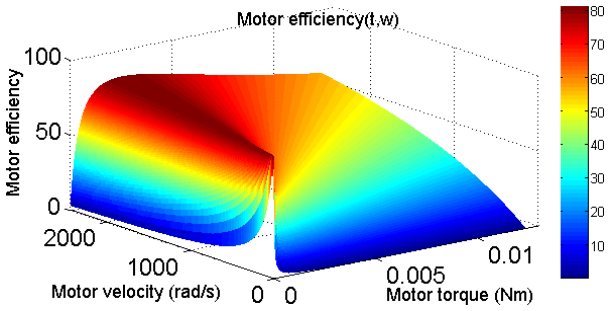

Fig. 1. Efficiency of servomotor HITEC HS-5955TG as a function of motor torque and speed.

of the motor M is linearly related to the maximum torque it can deliver. Both solutions will increase the mass drastically and this is highly detrimental for robots. Moreover, the required joint torques for robots increases with the size of the robot since the mass related forces (acceleration, gravity and impact forces) relate to L, the characteristic length of reference of a robot, by $M \approx L^3$ [11]. As a result, large robots require large joint torques, and thus large motors and gearboxes which is often hardly possible. Robots are far from outperforming the functionality and dexterity of humans.

On the contrary, the average power-to-weight ratio of a mammalian skeletal muscle (0.05 W/g) is much lower compared to electric motors (0.5 W/g), meaning an order of magnitude in favor of electric motors [12]. The maximum efficiency of an electric motor (>80%) is also higher than that of a muscle (<40%). Despite this higher power density and motor efficiency, an electric motor is not able yet to actuate mechatronic systems like biological muscles. Therefore, we believe the way transmissions and springs are used needs drastic innovation.

A first alternative to lower the motor torque is to implement a spring in parallel to a stiff actuator, often referred to as Parallel Elastic Actuation (PEA) [13]. Downside here is that the overall output is still a stiff actuator. A second approach is to place a spring in parallel to a SEA, as done by Herr in the powered ankle-foot prosthesis [14]. A disadvantage of passive springs in parallel to an actuator is that they limit movement dexterity. As the parallel spring is always engaged, these actuators tend to recoil the stored energy and induce joint motions that counter desired ones. Therefore we designed the innovative SPEA, presented in this paper, that allows lowered motor torque by variable recruitment and locking of parallel springs by means multiple dephased intermittent mechanisms in parallel.

III. SPEA with intermittent mechanism

The SPEA with an intermittent mechanism consists of a bundle of parallel compliant elements, typically springs, for which every spring can be contracted one after the other. A spring can be in three phases as shown in Fig. 2.B:

1) *In the unpretensioned phase,* the spring is at its rest length with its sides connected to both links;
2) *In the pretensioned phase,* the spring is extended with its sides connected to both links;
3) *In the pretensioning phase,* the motor controls the length of the spring and brings it from unpretensioned phase to pretensioned phase or back.

Only the forces that are exerted on the spring in the pretensioning phase will go through the motor. Since most of the springs are in the unpretensioned or the pretensioned phase, and only one or a few are in the pretensioning phase, only a fraction of the total force F_{Tot} exerted on the output link will be felt by the motor as indicated in Fig. 2.B. This is an advantage compared to a Variable Stiffness Actuator (VSA) where the F_{Tot} exerted on the output link will be felt entirely by the motor as indicated in Fig. 2.A.

The problem is then brought back to developing a

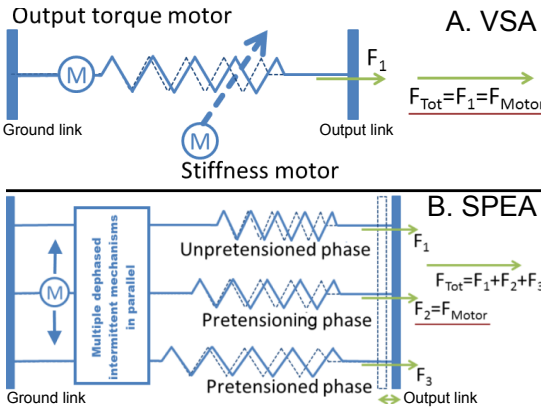

Fig. 2. Diagram of VSA and SPEA with intermittent mechanism to illustrate that for a VSA the $F_{motor} \cong F_{load}$ whilst for a SPEA this is only a fraction.

mechanism that, with a single motor, can achieve the springs to be in one of the three phases successively. The proposed solution in this paper is to use n parallel dephased intermittent mechanisms with internal locking. An intermittent mechanism transforms the continuous rotation of the motor to 2 consecutive phases: the motion period during which the spring controlled by the motor (i.e. in pretensioning phase) and the dwell period during which the spring is 'locked' (i.e. in pretensioned and unpretensioned phase). An intermittent mechanism with internal locking can be achieved with different mechanical principles [15]. However, designs that don't require an extra motor, don't induce large friction levels or shocks and that don't block when the output is under load are very rare. We have selected mutilated gears with a locking plate and ring as shown in Fig. 3.B and C. The basic concept of mutilated gears consists of removing a number of teeth on the driver of a pair of (spur) gears. As a result, the continuously turning driver only drives the driven output when the remaining teeth interact which results in an intermittent motion. The locking ring and

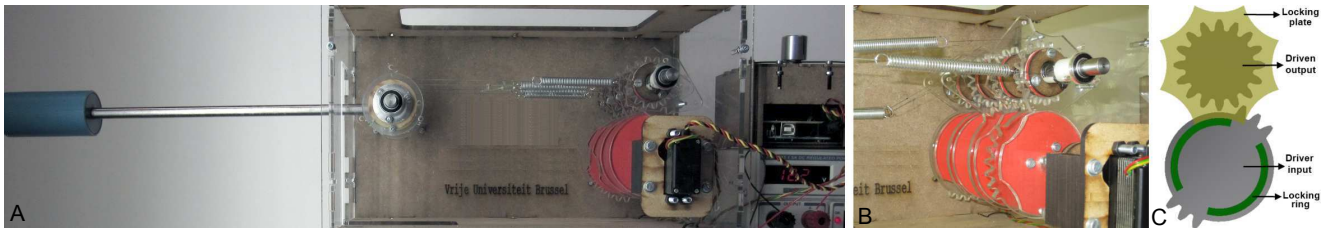

Fig. 3. From left to right: Overview picture of the PoC, a close-up of the mutilated gears and a scheme of one pair of mutilated gears.

plate lock the driven output during the dwell period.
In the SPEA, the driver inputs of the mutilated gears are fixed to the motor input axis and the driven outputs are each connected to a spring. Since the driven inputs are dephased relative to one another, the total mechanism enables to tension and lock the n parallel springs in the SPEA successively. The PoC scheme in Fig. 4 clarifies the above reasoning.
Mutilated gears block at the transition from the dwell period to the motion period, when the load on the driven output is in the same rotational direction as the motion of the driver. To bypass this problem, we tension each spring from the singular position of no torque at the lever arm at 0° to the next singular position over 180° (as can be seen in Fig. 4 where ϕ_1 and ϕ_2 are locked at -180°). As a result, the transition from dwell period to motion period is without any load on the output and the mechanism doesn't block. A second advantage of locking in a singular position of no torque at the lever arm, is the reduction of friction levels in the dwell period between the locking ring and plate. Mutilated gears offer design freedom regarding the motion curves since the length of the dwell period (and possibly multiple dwell periods) depends on the number of teeth removed. Furthermore, since mutilated gears are adapted normal gears, the gear ratio can still be chosen and the efficiency is high. The main disadvantage is the impact produced at the start of every motion period.
Inspiration for the SPEA concept is found in the microscopic structure of skeletal muscle, which consists of a large set of parallel and series motor units. The force produced by a single motor unit is partly determined by the number of muscle fibres in the unit. A muscle can be progressively activated by successive motor unit recruitment [16]. In order to lift a light object only a small number of motor units are recruited, while more motor units are recruited to lift a heavier object. These biological findings provide a logic amenability for the unconventional and challenging study of the SPEA concept.

IV. Proof of Concept

The working principle of the PoC (shown in Fig. 3) is elaborated in this section, followed by the theoretical model that describes the PoC. The PoC consists of 4 parallel springs, which is sufficient to demonstrate the working principle, whereas more springs would further decrease the maximum motor torque. The springs in the PoC are turned to the pretensioned phase one by one in order to increase the generated torque T_{SPEA}. The most important parameters are shown in Fig. 4 and listed in section IV-B. Please also see the video accompanying this paper for further clarification of the working principle.

A. Working principle and realization

The PoC consists of 4 dephased mutilated gear mechanisms, each having one motion period and one dwell period. The driver of each parallel mutilated gear mechanism is fixed to the input shaft, which is connected to the servomotor, as indicated in Fig. 4. The driven outputs of the mutilated gear mechanisms are connected to a lever arm which is mounted on the lever arm shaft. During a dwell period the driven output is locked (due to the locking plate and locking ring), while during a motion period the driver actuates the driven output, which acts like a lever arm. Each spring is connected with a wire to one of the lever arms on the input side and to one of the drums on the output side. Since the wires are wrapped around one side of the drums, the output torque is unidirectional.
As explained before, the springs in both unpretensioned and pretensioned phase are locked in a singular position of no torque at the lever arm. This means that each of the lever arms should be turned 180° during motion period. Since the PoC consists of 4 lever arms that each should turn 180°, the gear ratio of the mutilated gear mechanisms should be $\epsilon = \frac{1}{2}$ so that the driver shaft of the mutilated gear mechanism has to turn 360° in order to tension all 4 springs.
By leaving enough space between the springs and using Plexi sides cut by laser, a clear demonstrator is obtained that can be converted to an SPEA with 2 springs or SEA. Dimensions can be scaled down for implementation in applications. An Arduino board with custom-design PCB is used to control the device and perform the measurements. The servomotor is a HITEC HS-5955TG coreless digital servomotor with a 4-stage titanium gearbox. The servomotor is modified to enable continuous rotation. A current sensor (ACS712 fully integrated, Hall effect-based linear current sensor IC) is installed over the DC motor poles as well as a voltmeter, to measure the consumed electric motor power and calculate the motor torque. The gravitational output torque can be calculated indirectly since the output angle ψ is known by measurement, as well as the mass connected to the

output arm and the length of the output arm. Each of the four springs in the SPEA has a stiffness of $350\frac{N}{m}$ and rest length $0.05\,m$.
It is important to note that in this agonistic set-up the springs in the unpretensioned phase clearly sag as shown in Fig. 4. The unpretensioned springs are at rest length at $\phi_i = 0$. When the output angle $\psi \neq 0$ the unpretensioned springs sag. As a result, the compliance regarding the output is not equal to $n * \frac{k}{n} = k$ but smaller. The effect of sagging springs will also be implemented in the theoretical model here underneath.

B. Theoretical model

In this section all equations needed to calculate the motor torque $T_{SPEA\,motor}$ and motor velocity $\omega_{SPEA\,motor}$, w.r.t. a certain required torque T_{req} and angular velocity ω_{req} profile at the output, will be derived for the PoC. The following list contains all relevant parameters of the PoC as indicated in Fig. 4:

- n = number of springs in parallel;
- ϕ = motor input angle;
- ψ = output angle;
- k/n = spring constant of one spring in a SPEA set-up with n springs;
- L_{lever} = input lever arm length;
- D_{out} = output drum diameter;
- $L(\phi_i)$ = distance from both connection points, tip lever arm and outside of output drum, of the wires of spring i. Is dependent on ϕ_i and thus ϕ;
- H = horizontal distance between motor axis and output axis;
- $\epsilon = \frac{1}{2}$;
- $T_{SPEA\,motor}$ = motor torque;
- $\omega_{SPEA\,motor}$ = angular motor velocity;
- T_{SPEA} = torque applied by the PoC.

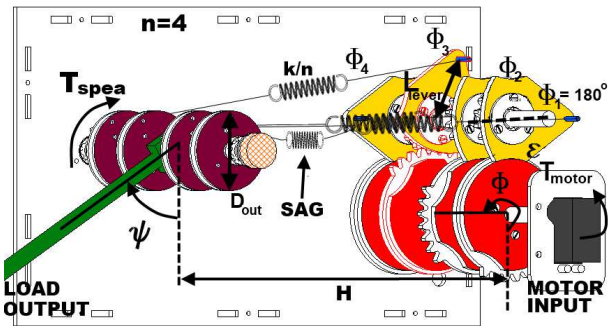

Fig. 4. Scheme with all relevant parameters of the PoC.

For a certain input motor angle ϕ, all input lever arms are positioned at specific angles ϕ_i (ϕ_1 to ϕ_n). The angular position of the lever arm that is actuated by the motor, ϕ_{actual}, depends on the motor angle ϕ and on the design of the mutilated gears. Expressions for both ϕ_{actual} and ϕ_i can be found in (3) and (4). Abs(x) stands for the absolute value of x. Furthermore, $\frac{x+abs(x)}{2}$ returns x when x is positive and returns 0 when x is negative or 0. Function Fix(x) rounds x to the nearest integer towards zero.

$$\phi_{actual}(\phi) = \frac{-1}{\epsilon}\left(\phi - fix\left(\frac{\phi}{\frac{2\,\pi}{n}}\right)\frac{2\,\pi}{n} + fix\left(\frac{fix\left(\frac{\phi}{\frac{2\,\pi}{n}}\right)}{n}\right)\frac{2\,\pi}{n}\right) \tag{3}$$

$$\phi_i(\phi) = \left(\frac{\phi - (i-1)\frac{2\pi}{n} + abs\left(\phi - (i-1)\frac{2\pi}{n}\right)}{2} + \frac{2\pi}{n}\right)\frac{1}{2} - abs\left(\frac{\phi - (i-1)\frac{2\pi}{n} + abs\left(\phi - (i-1)\frac{2\pi}{n}\right)}{2} - \frac{2\pi}{n}\right)\frac{1}{2} \tag{4}$$

Analogous to ϕ_{actual} and ϕ_{i}, Ext_{actual} and Ext_{i} are defined for the spring extensions in (5) and (6).

$$Ext_{actual}(\phi, \psi_{req}) = \left(L\left(-\epsilon\phi_{actual}(\phi)\right) + L_{lever} - H + \frac{\psi_{req} D_{out}}{2}\right)\frac{1}{2} - abs\left(L\left(-\epsilon\phi_{actual}(\phi)\right) + L_{lever} - H + \frac{\psi_{req} D_{out}}{2}\right)\frac{1}{2} \tag{5}$$

$$Ext_i(\phi, \psi_{req}) = \left(\left(L\left(\phi_i(\phi, i)\right) + L_{lever} - H + \frac{\psi_{req}\, D_{out}}{2}\right) - abs\left(L\left(\phi_i(\phi, i)\right) + L_{lever} - H + \frac{\psi_{req}\, D_{out}}{2}\right)\right)\frac{1}{2} \tag{6}$$

All the above mentioned parameters will now be used to calculate the motor angular position $\phi_{SPEA\,motor}$, the motor angular velocity $\omega_{SPEA\,motor}$ and the motor torque $T_{SPEA\,motor}$ as a function of the desired output torque T_{req} at desired output angle ψ_{req}. The motor angular position $\phi_{SPEA\,motor}$ can be found by (7):

$$T_{req} = \sum_{i=1}^{n} -\frac{k}{n}\frac{D_{out}}{2} Ext_i(\phi, \psi_{req}) \tag{7}$$

Derivation of $\phi_{SPEA\,motor}$ leads to $\omega_{SPEA\,motor}$. The motor torque $T_{SPEA\,motor}$ can now be found by means of (8) and $\phi_{SPEA\,motor}$ which was found by (7):

$$T_{SPEA\,motor} = \frac{1}{\epsilon}\frac{k}{n} \sin\left(\beta(-\epsilon\,\phi_{actual}(\phi))\right) L_{lever}\, Ext_{actual}(\phi, \psi_{req}) \tag{8}$$

V. Experimenal results

In this section, we present the results of the experiments conducted on the PoC. We aim to validate the SPEA model with the experiments. Furthermore, the results will show the lowered motor torque and increased efficiency of the SPEA compared to other actuation schemes.

A. Motor torque experiments

The first experiment aims to show the lowered motor torque of the SPEA compared to an equivalent stiff actuator and SEA. In Fig. 6 the respective motor torques are plotted as a function of the output angle ψ of the actuators. The output is connected to a gravitational load of 0.26 kg at 0.3 m which will be lifted to its horizontal position at 90 °. Since the output torque is in sinusoidal relation to the output angle, the motor torque of the stiff actuator is a sinus. The motor torque of the SEA has a comparable maximum, since both actuators are serial set-ups, and ends at 0 Nm since the lever arm is locked in a singular position at 90 °. The modeled SPEA motor torque is clearly lower than both serial set-ups. The measured SPEA torque in the red dotted curve of Fig. 6 consists of 4 humps that logically resemble a scaled SEA curve since each of the lever arms is locked in a singular position of no torque. The decrease in the successive 4 maxima is caused by the sagging of the springs.
The motor torque was measured for output angles up to 90 ° with 1 ° intervals. Each measurement is done at constant motor angle ψ, which means the measured motor current I is directly related to the motor torque, since $\omega_{\text{motor}} = 0$ in (1). The measured SPEA motor torque approximates the model. The total torque produced by the pretensioned springs rises and equals the total output torque when the output angle is at 90 ° and all springs are tensioned and locked.

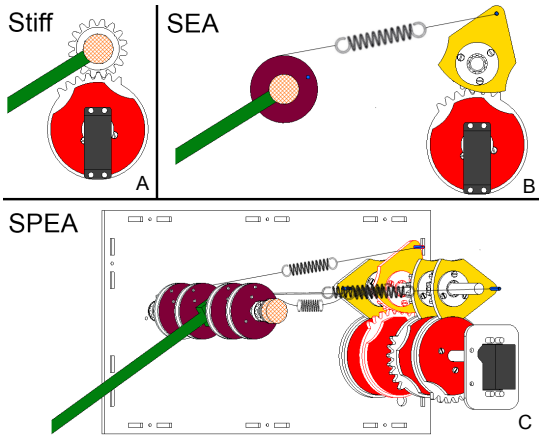

Fig. 5. The SPEA with 4 springs and equivalent SEA and stiff actuator.

B. Motor power and efficiency experiments

For the second experiment, measurements on both the SPEA and equivalent stiff actuator are performed. Both actuators lift the gravitational load of 0.26 kg at 0.3 m (equal as for the torque experiment). Since the stall torque of the servomotor is 2.35 Nm (and the holding torque 3 Nm) the stiff actuator is not able to lift the weight completely to the horizontal position at 90 ° and 3 Nm, as can be seen on Fig. 6. Therefore the load is lifted to 1.2 rad or 2.7 Nm in 14 s. Both actuators produce the same mechanical power at the output since they track the same trajectory over time. The average trajectories of 4 measurements are shown in Fig. 7.A. The standard deviation is smaller than the line width and thus not plotted.

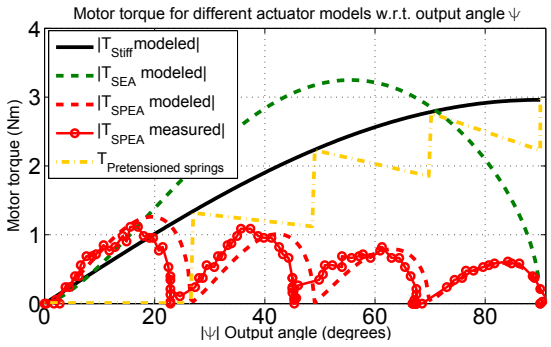

Fig. 6. Motor torque measurement of the SPEA with 4 springs when lifting a gravitational load to horizontal position at 90 °. The SPEA torque measurements match the modeled trend of reduced motor torque. Models of stiff and SEA equivalent actuators are shown for comparison.

The current and voltage of the motor in both actuators are measured and their product gives the measured electric power consumed by the motor. Again, the curves with measured data in Fig. 7.B are both the average of 4 measurements. The standard deviation is plotted in thin lines around the measured data. The motor data and (1) enable to calculate the required motor torque and velocity based on the required output trajectory. The electric motor power curves from the model of the stiff actuator and the SPEA are plotted on top of the measurements in Fig. 7.B. The measurements and the model clearly follow the same trend, namely the fact that the consumed electrical power of the stiff actuator increases rapidly with increased output torque. In contrast, the electrical power of the SPEA is lower and more constant with increasing output torque

Since the mechanical power at the output is equal for both the stiff actuator and the SPEA, and since the electrical power is higher for the stiff actuator, the efficiency of the SPEA is higher than that of the stiff actuator. This is because the motor is used in a more efficient region of the speed-torque graph of Fig. 1. To indicate this, Fig. 7.C shows the motor efficiency of both actuators during the experiment. Although the motor speed of the SPEA is increased, since more than one spring needs to be tensioned, the motor torque is lowered. Therefore, the motor of the SPEA is clearly used in a more efficient region during the whole experiment.

VI. Conclusions and Future Work

In this paper, we introduced the novel SPEA compliant actuation concept based on an intermittent mechanism where parallel springs are variably recruited. The experiments on the PoC showed that the SPEA concept can drastically lower the required motor torque and as such

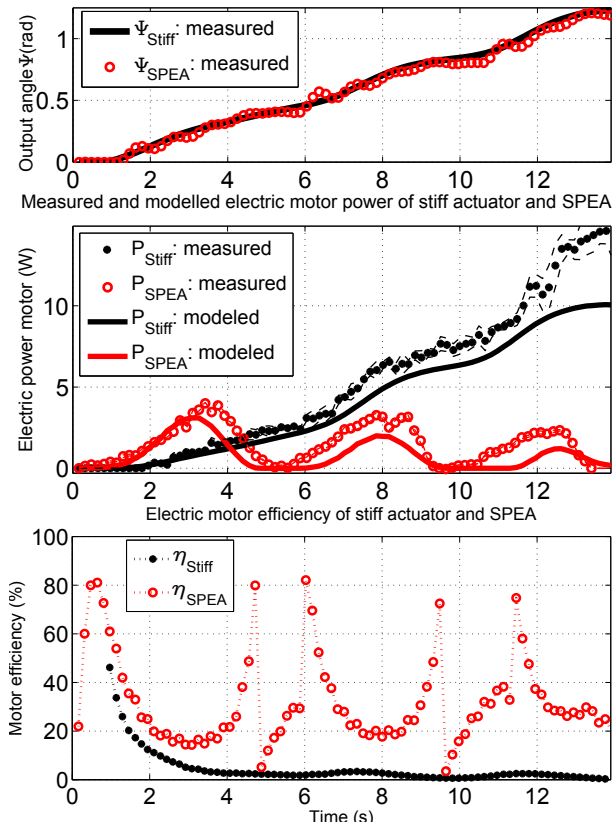

Fig. 7. The stiff actuator and SPEA clearly track the same trajectory over time. The measurements and the model indicate the increased efficiency of the SPEA compared to the stiff actuator.

use the DC motor in a more efficient working range, while maintaining the inherent compliance.

Future work consists of the work on a novel detent-latching mechanism to replace the mutilated gears. This will allow bidirectional output torque and the implementation of variable compliance as was done for the SEA. Since the overall output stiffness of a SPEA is equivalent to a SEA, we expect to use the same control strategies developed for compliant actuators, for example to avoid oscillations by damping control, exploit natural dynamics for cyclic motions, etc. depending on the targeted application. Currently for the PoC, an open-loop controller is used.

Undiscussed so far are the increase in complexity and the potential increase in mass and volume of the SPEA, compared to stiff actuators and SEAs, as potential drawbacks. We strongly believe that these drawbacks are instant since modern production techniques (such as 3D multi-material printing) are evolving at a speed which eliminates the increased complexity bottleneck. Furthermore, a SPEA with n springs will not necessarily weigh more than a SEA. There are indeed n dephased intermittent mechanisms, but these can be downgraded since they are only subjected to a fraction of the total output torque. The size and weight of the PoC are currently unoptimized.

We hope that this novel actuation concept, based on the working principle of a skeletal muscle, provides the impulse for research towards more efficient actuators for the robots of tomorrow.

ACKNOWLEDGMENT

This work has been funded by the European Commission 7th Framework Program as part of the project H_2R (no.600698) and ERC-grant SPEAR (no.337596).

REFERENCES

[1] A. Albu-Schaffer, O. Eiberger, M. Grebenstein, S. Haddadin, C. Ott, T. Wimbock, S. Wolf, and G. Hirzinger, "Soft robotics," *Robotics & Automation Magazine, IEEE*, vol. 15, no. 3, pp. 20–30, 2008.

[2] Hogan, "Impedance control: An approach to manipulation," in *American Control Conference, 1984*, 1984, pp. 304–313.

[3] G. A. Pratt and M. M. Williamson, "Series elastic actuators," in *IEEE/RSJ International Conference on Intelligent Robots and Systems (IROS)*, vol. 1. IEEE, 1995, pp. 399–406.

[4] R. Alexander, "Three uses of springs in legged locomotion," *International Journal of Robotics Research (Special Issue on Legged Locomotion)*, vol. 9, no. 2, pp. 53–61, 1990.

[5] R. Van Ham, T. Sugar, B. Vanderborght, K. Hollander, and D. Lefeber, "Review of actuators with passive adjustable compliance/controllable stiffness for robotic applications," *Robotics & Automation Magazine*, vol. 16, no. 3, pp. 81–94, 2009.

[6] A. Jafari, N. Tsagarakis, and D. G. Caldwell, "Awas-ii: A new actuator with adjustable stiffness based on the novel principle of adaptable pivot point and variable lever ratio," in *Robotics and Automation (ICRA), 2011 IEEE International Conference on*. IEEE, 2011, pp. 4638–4643.

[7] S. Groothuis, G. Rusticelli, A. Zucchelli, S. Stramigioli, and R. Carloni, "The vsaUT-II: A novel rotational variable stiffness actuator," in *Robotics and Automation (ICRA), 2012 IEEE International Conference on*. IEEE, 2012, pp. 3355–3360.

[8] N. L. Tagliamonte, F. Sergi, D. Accoto, G. Carpino, and E. Guglielmelli, "Double actuation architectures for rendering variable impedance in compliant robots: A review," *Mechatronics*, vol. 22, no. 8, pp. 1187 – 1203, 2012.

[9] G. Mathijssen, P. Cherelle, D. Lefeber, and B. Vanderborght, "Concept of a series-parallel elastic actuator for a powered transtibial prosthesis," *Actuators*, vol. 2, no. 3, pp. 59–73, 2013.

[10] J. H. Marden, "Scaling of maximum net force output by motors used for locomotion," *Journal of Experimental Biology*, vol. 208, no. 9, pp. 1653–1664, 2005.

[11] G. Caprari, T. Estier, and R. Siegwart, "Fascination of down scaling alice the sugar cube robot," *Journal of micromechatronics*, vol. 1, no. 3, pp. 177–189, 2001.

[12] J. Madden, N. Vandesteeg, P. Anquetil, P. Madden, A. Takshi, R. Pytel, S. Lafontaine, P. Wieringa, and I. Hunter, "Artificial muscle technology: physical principles and naval prospects," *IEEE Journal of Oceanic Engineering*, vol. 29, no. 3, pp. 706 – 728, july 2004.

[13] M. Grimmer, M. Eslamy, S. Gliech, and A. Seyfarth, "A comparison of parallel-and series elastic elements in an actuator for mimicking human ankle joint in walking and running," in *2012 IEEE International Conference on Robotics and Automation (ICRA)*. IEEE, 2012, pp. 2463–2470.

[14] S. K. Au, J. Weber, and H. Herr, "Powered ankle–foot prosthesis improves walking metabolic economy," *IEEE Transactions on Robotics*, vol. 25, no. 1, pp. 51–66, 2009.

[15] J. Bickford, *Mechanisms for intermittent motion*. Industrial Press New York, 1972.

[16] E. Henneman, "Relation between size of neurons and their susceptibility to discharge," *Science*, vol. 126, no. 3287, pp. 1345–1347, 1957.